International Journal of Mass Spectrometry 308 (2011) 225–231

Contents lists available at ScienceDirect

International Journal of Mass Spectrometry

journal homepage: www.elsevier.com/locate/ijms

Investigating the gas phase structure of KIX with radical directed dissociation and molecular dynamics: Retention of the native structure

Xing Zhang, Ryan R. Julian*

Department of Chemistry, University of California, Riverside, CA 92521, United States

ARTICLE INFO

Article history:
Received 11 May 2011
Received in revised form 7 July 2011
Accepted 11 July 2011
Available online 20 July 2011

Keywords:
Electron capture dissociation
Ion mobility
Tertiary structure
α Helix
Photodissociation

ABSTRACT

Evaluating protein structure in the gas phase is useful for understanding the intrinsic forces which influence protein folding and for determining the feasibility of probing condensed phase structure with gas phase interrogation. KIX is a three-helix bundle protein that has been reported previously to preserve the condensed phase structure in the gas phase. Herein, structure dependent radical directed dissociation (RDD) is used to examine the gas phase structure of KIX by establishing residue specific distance constraints which can be used to assess candidate structures obtained from molecular dynamics simulations. The data obtained by RDD is consistent with KIX structures that largely retain condensed phase structure as determined previously by NMR. There are several factors that favor retention of the KIX native fold in the gas phase. The structure is largely comprised of alpha helices, which are known to be stable in the gas phase. This is particularly true if the C-terminus of the helix is capped with a positive charge, which occurs for the two most stable helices in KIX. There are several arginine based salt bridges which link critical portions of KIX together. KIX also has an abundance of basic residues; this multiplicity increases the chance that sites which require little structural reorganization following desolvation can be charge carriers. Thus under appropriate conditions, solution phase structure can be largely retained and meaningfully examined in the gas phase.

1. Introduction

Protein structure is a subject of intense interest in a variety of different contexts [1]. From a chemical perspective, determination of protein structure is one of the primary prerequisites for understanding (and ultimately controlling) functionality. Ideally protein structure should be examined within the framework of conditions that are present in cells where proteins carry out their various duties [2]. In reality, all experimental methods for examining protein structure fall short in this regard, although arguably some are closer than others. The gas phase is not typically an environment which is considered to be similar to a cell, yet methods for examining protein structure in the gas phase continue to increase in popularity, including those utilizing mass spectrometry, ion mobility, and spectroscopy [3,4]. Reasons for this are clear, gas phase experiments can be carried out rapidly with minimal sample consumption [5]; therefore, proteins which are present in very small abundance can be targeted. Perhaps even more importantly, several gas phase techniques can easily accommodate increasing protein size, allowing for the interrogation of large systems [6]. However, despite the increasing popularity, it is more difficult to ascertain whether the information obtained in the gas phase is relevant to the condensed phase, and if so, under what conditions.

Ion mobility is the most frequently used method for examining the structures of large molecules in the gas phase [7–12]. Although there are now several varieties of experimental setups, all utilize electric fields and a buffer gas to separate ions according to their average collision cross section or "size". This experimentally determined parameter can be used to evaluate candidate structures, typically derived from molecular dynamics simulations. The strengths of the ion mobility approach include direct measurement of a structural parameter and the ability to easily accommodate increasing molecular size. It is equally easy to measure the collision cross section of a small peptide or a large protein. The primary disadvantage of ion mobility is that only a single parameter (collision cross section) can be obtained, regardless of the experimental setup. Constraining all of protein structural space with a single parameter can be quite challenging.

Electron capture dissociation (ECD) has also been used to investigate protein structure [13–15]. In these experiments, it is assumed that dissociation into c/z ions occurs throughout the protein backbone. Failure to observe fragmentation is interpreted to signify that noncovalent interactions are holding the two fragments together.

* Corresponding author.
E-mail address: ryan.julian@ucr.edu (R.R. Julian).

1387-3806/$ – see front matter © 2011 Elsevier B.V. All rights reserved.
doi:10.1016/j.ijms.2011.07.010

The noncovalent interactions could originate from secondary or tertiary structural features. With ECD, it is possible to map out which portions of a protein have the least contact with the remaining structure as a function of the charge state. The relative stability of structural features can in theory be mapped this way because all proteins adopt more elongated structures in the gas phase as the charge state increases. Unfortunately, for compact structures which are frequently most likely to be similar to those found in solution, little information is obtained by ECD since the primary observation is simply lack of fragmentation. Similarly, this method cannot distinguish between close contacts which are strongly interacting with one another and contacts which are merely in close proximity, but not strongly interacting.

Radical directed dissociation (RDD) is a new method which can examine protein structure [16]. In these experiments, radical precursors are placed site specifically at particular residues within a protein. Photodissociation is then used to generate a radical by homolytic cleavage of a photolabile carbon–iodine bond. The initially formed radicals are reactive, but not well placed to induce dissociation [17]. Thus migration of the radical species to locations where dissociation is favorable occurs rapidly [18]. Mild collisional activation can then be used to facilitate fragmentation, and the locations of the radical directed dissociation sites can be easily determined by evaluation of the fragments which are produced. In this fashion, a series of distance constraints between radical initiation and termination points can be determined and used to evaluate candidate structures. Ideally, the distance constraints can be used to actually drive molecular dynamics simulations towards relevant conformational space [16]. Multiple structure parameters are obtained in a typical experiment, and compact structures can be investigated along with extended conformations. The primary drawback for this methodology is that the protein must be modified, and that structure will only be probed in the vicinity of the site of modification. Iodination of the most reactive tyrosine residue is simple [19] and the preferred starting point for RDD structure probing. Of course, modification at additional sites is possible for most proteins, but only at the cost of significant efforts to install other modifications site specifically [20].

KIX is a three-helix domain within the larger CREB binding protein which is involved in the regulation of transcriptional processes [21]. The KIX domain itself is a recognition motif, which can bind simultaneously to two other proteins to form a ternary complex. The structure of KIX has been investigated by both NMR in solution [22] and in the gas phase by ECD [23]. Evaluation of the ECD data suggested that the solution phase structure of KIX is largely retained in the gas phase and stable for at least 4 s due to favorable electrostatic interactions. This conclusion was primarily based on evaluation of data related to secondary structure from high charge states (+10 or larger), which likely represent more extended conformations of the protein. For reasons explained above, examination of the structure of the lower charge states was not possible.

Herein, RDD is used to examine the gas phase structure of KIX in the +6 and +7 charge states. Comparison with the solution phase structure reveals that the RDD data is consistent with the solution phase structure being largely retained in the gas phase. Exploration of potential alternate structures based on the RDD data by molecular dynamics failed to yield any substantially lower energy structures. KIX is a three-helix bundle protein, with the helices connected by fairly flexible linkers. Desolvation of KIX is accompanied by only slight shifting of the helical regions to accommodate charge solvation. KIX contains a high density of basic and acidic residues, which is important for several reasons. It enables the formation of favorable electrostatic interactions, as noted previously [23]. Furthermore, when charges are placed on the protein, there are numerous options. This multiplicity may be important in allowing the protein to acquire a net charge at locations which do not require significant structural reorganization.

2. Experimental methods

2.1. Materials

KIX domain from CREB binding protein was expressed in *Escherichia coli* cells using a plasmid that includes residues 586–672, with residue 586 corresponding to residue 5 here. KIX was provided as a generous gift by Dr. Kathrin Breuker and Dr. Martin Tollinger. α-Cyano-4-hydroxycinnamic acid (CHCA) and trypsin (porcine pancreas) were purchased from Sigma–Aldrich (St. Louis, MO). Lysyl endopeptidase (Lys C) and endoproteinase Asp N were purchased from Wako Chemicals, USA (Richmond, VA). Methanol, glacial acetic acid, sodium iodide, chloramine-T, sodium metabisulfite were purchased from Fisher Scientific (Fairlawn, NJ).

2.2. Iodination of protein

Ortho position of tyrosine side chains in KIX protein were iodinated by sodium iodide and chloramine-T at room temperature, after a short reaction time of about 10 min, excess sodium metabisulfite was added to quench the reaction. Diluted solution (10 μM protein) and stoichiometric quantities of reagents (1:2:1:2 molar ratio of KIX/sodium iodide/chloramine-T/sodium metabisulfite) were used to limit the iodination extent and produce mainly mono-iodinated KIX. Iodinated KIX was then purified by a desalting trap (Michrom Bioresources, Inc., Auburn, CA) to remove excess iodination reagents.

2.3. Enzymatic digestion

Iodinated KIX was digested by trypsin, endopeptidase Asp N or Lys C separately in 20 μL 50 mM sodium bicarbonate buffer at 37 °C overnight. Enzyme to substrate ratio 1:10 (w/w) was used. The protein cleavage was stopped by adding 0.1 μL trifluoroacetic acid to a final concentration of 0.5% (v/v). Digested mixtures were desalted with C_{18} ZipTip (Millipore, Billerica, MA) and then directly eluted onto a MALDI sample plate. CHCA was used as matrix for on plate mixing. MALDI-TOF analysis was carried out with Voyager-DE STR mass spectrometer (Applied Biosystems, Framingham, MA), equipped with a 337 nm nitrogen laser. The spectra were averaged and recorded in the positive reflector mode at an accelerated voltage of 20 kV in the range from 500 to 3500 Da.

2.4. Photodissociation

Iodinated KIX (2 μM) in 80:20 H_2O:CH_3OH with 0.1% acetic acid was electrosprayed into an LTQ linear quadrupole ion trap mass spectrometer (Thermo Fisher Scientific, San Jose, CA). The back plate of the instrument was modified with a quartz window to transmit 266 nm UV photons into the linear ion trap, from the 4th harmonic generation of a Nd:YAG laser (Continuum, Santa Clara, CA). Laser pulses were synchronized to the isolation step via a digital delay generator. Charge state of fragments after collision activated dissociation (CAD) were assigned using the zoom or ultrazoom scan modes, which can typically resolve isotope peaks of up to +8 charge state. Protein fragments were assigned manually with the aid of Fragmentor 1.2.2 (http://www.faculty.ucr.edu/~ryanj/fragmentor.html) and UCSF ProteinProspector program v.5.7.3 (http://prospector.ucsf.edu/prospector/mshome.htm). Assignments do not distinguish between even electron fragments vs. radical fragments with only 1 Da difference.

2.5. Molecular modeling

MacroModel, version 9.9, Schrödinger, LLC, New York, NY, molecular mechanics software package was used to build models of charged KIX, calculate surface accessibility, and perform all molecular modeling simulations. The OPLS force field [24] and constant dielectric electrostatic, $\varepsilon = 1.0$, was used for all calculations. Extended cutoffs were used for dipole–dipole interactions. Energy minimization was performed using the Polak-Ribiere Conjugate Gradient [25] method with a derivative convergence criterion of 0.05 kJ/Å mol. The initial "seed" structure was taken from KIX domain in a complex determined by NMR (2AGH) [22] For the +6 charge state of KIX, different sets of charge sites were assigned to explore the importance of charge location. The following groups of residues were either protonated or deprotonated as appropriate to yield a +6 charge state: (R7, R42, R65, R90, K53, K75), (R7, R19, R42, R65, R90, K75), (R7, R42, R90, K25, R53, R75), (R7, R19, R42, R65, R87, R90), (R7, R19, R42, R43, R65, R87, R90, E55), (R7, R19, R42, R88, R90, K8, K53, K75, K81, D41, E55, C-terminus). All other residues were uncharged. Constrained molecular dynamics and multiple cycles of simulated annealing were used to explore more conformation space as described in the text below.

3. Results and discussion

3.1. Localization of iodinated tyrosine

To obtain information about protein structure through radical migration and dissociation, the initial radical site should ideally be known. In the present work, radicals are generated by photodissociation of carbon–iodine bonds present in iodinated tyrosine residues. In order to favor single site modification, iodination was carried out under mild conditions which produce primarily mono-iodinated KIX and avoid histidine modification. KIX contains five tyrosine residues with Tyr50 and Tyr59 in the α2 helical region, and Tyr68, Tyr69 and Tyr77 in α3. Based on aqueous NMR structures, Tyr68 is buried inside the three-helix bundle and Tyr59 is partially buried, while the other three tyrosines are well exposed at the surface. The surface accessibilities to iodine as calculated from the NMR structure for each tyrosine residue are shown in Table 1. Previous work has shown that solvent accessibility alone cannot determine probability of iodination [19], presumably due to the influence of other factors within the local chemical environment surrounding the tyrosine side chain such as intramolecular hydrogen bonds or salt bridges.

Identifying the site of iodination for mono-iodinated KIX is not achievable by simple CAD of the entire protein due to incomplete sequence coverage and numerous uninformative fragmentation pathways. Instead, enzymatic digestion of the mixture of unmodified, mono- and multiple-iodinated KIX was carried out. MALDI-MS was used to analyze the proteolytic digest fragments. The results are summarized in Fig. 1. The bar height represents the iodination extent for each tyrosine, which is determined by the ratio of the relative intensity of the mono-iodinated to non-iodinated peptide. If the corresponding peptide fragment was not observed, then the bar is absent in Fig. 1. Those bars with a value of zero indicate a measured quantity. Three enzymes, trypsin, Lys C and Asp N were each used in an effort to increase the sequence coverage

Table 1
Surface accessibility (Å^2) of tyrosine side chain defined at 1.4 Å van der Waals sphere.

	Tyr50	Tyr59	Tyr68	Tyr69	Tyr77
Two ortho carbon atoms	10.8	3.7	0.0	12.7	14.6
Phenol ring	85.3	29.8	0.0	78.5	134

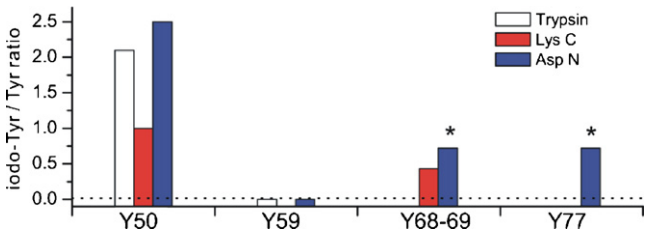

Fig. 1. Iodination extent at each tyrosine in KIX quantified by MALDI analysis of enzyme digested iodinated KIX. * Indicates a peptide containing Tyr68, Tyr69 and Tyr77.

and to obtain overlapping results. Although the final results are semi-quantitative, Tyr50 is obviously the primary iodination site. Tyr59, which is partially buried inside the three-helix bundle, is not iodinated at all. Tyr68 and Tyr69 cannot be distinguished as both are present in all digested peptides, therefore they are grouped together as one potential iodination site. Tyr77 was only observed in the Asp N digestion, but the relevant peptide in that case also includes Tyr68 and Tyr69, confounding independent analysis. Considering that Tyr68 and Tyr69 are partially iodinated as shown by the results obtained with Lys C, it is likely that Tyr77 may only be iodinated to a small extent. It is important to point out that the digestion results include some information about secondary sites of iodination as the doubly iodinated species could not be separated out prior to analysis. In summary, Tyr50 in KIX is the likely primary iodination site, Tyr68–69 and Tyr77 may also be iodinated to a smaller extent. These results are in agreement with those obtained by photodissociation, which has been demonstrated previously to provide iodination site identification in very high charge states [19].

3.2. Radical directed dissociation (RDD)

The iodinated KIX mixture was electrosprayed from a solution of 80:20 H_2O:CH_3OH with 0.1% acetic acid. The mono-iodinated KIX

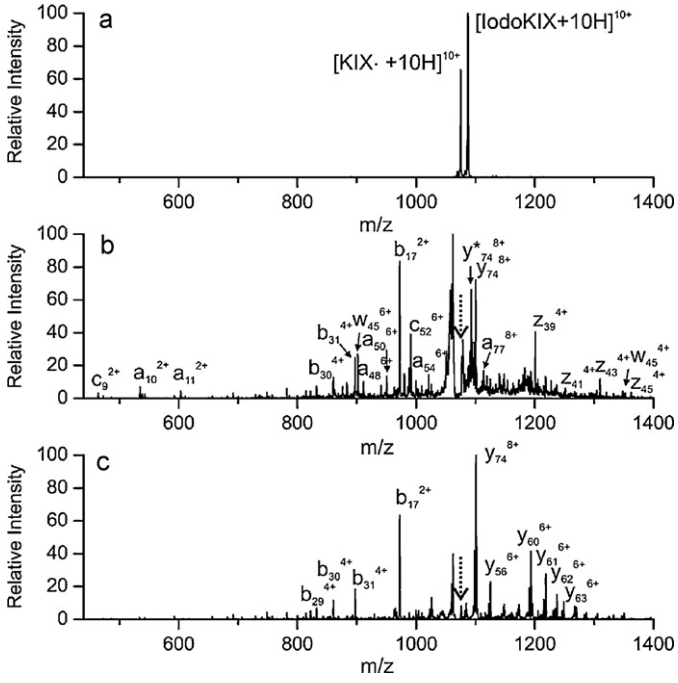

Fig. 2. (a) Photodissociation of the +10 charge state of iodo-KIX generates odd electron KIX radical. (b) CAD of the KIX radical from (a) generates radical directed fragment ions (backbone a, c/z, w series and side chain loss peaks) and also some proton directed b/y fragments. (c) CAD of the even electron +10 KIX generates mainly b/y fragments. * Represents side chain loss from the corresponding fragment.

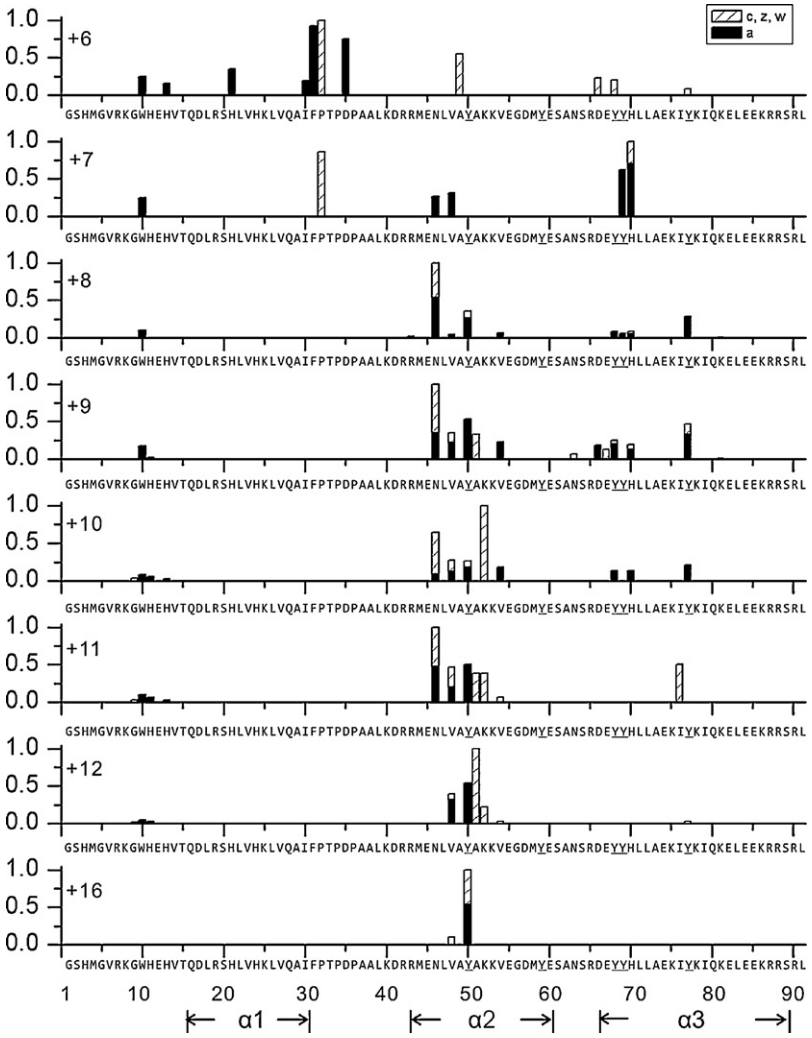

Fig. 3. Relative abundance of fragments resulting from radical directed backbone dissociation of KIX along the amino acid sequence in different charge states. The sum of fragments at each residue is normalized to the highest sum.

was then isolated in the ion trap and subjected to photodissociation with a single pulse of 266 nm photons, which led to homolytic cleavage of the carbon–iodine bond as shown in Fig. 2a for the +10 charge state. After loss of I•, a radical is generated at tyrosine side chain. The CAD spectrum of this re-isolated +10 protein radical is shown in Fig. 2b. Radical initiated a, c, w, and z fragment ions are produced as well as some abundant proton initiated b/y ions. These b/y ions are also produced by CAD of the even-electron +10 KIX as shown in Fig. 2c, in addition to several other b/y ions. RDD of peptides frequently occurs at a lower dissociation threshold than proton initiated dissociation, but some of the proton initiated pathways are competitive in CAD of radical KIX protein. The most abundant fragmentation channel in CAD of radical +10 KIX is non-radical initiated cleavage of Asp17/Leu18 to produce b_{17}/y_{74} ions, presumably due to the aspartic acid effect [26]. Other competitive fragmentations such as those yielding the b_{31}/y_{60} and b_{35}/y_{56} ion pairs occur at proline [27]. Most of the remaining proton initiated dissociation pathways observed in Fig. 2c are substantially suppressed in Fig. 2b. Similar results and conclusions can be drawn for most other charge states of KIX.

The radical can migrate from the initial tyrosine side chain to other specific residues, leading to subsequent dissociation (e.g., β-scission) at those residues. RDD of proteins can result in both backbone dissociation (e.g., a50, c52, w45, z39 in Fig. 2b) and various side chain losses. The broad peak with a trailing edge at lower *m*/*z* in Fig. 2b results from overlapping (and sometimes multiple) side chain losses from the radical precursor. These side chain loss peaks are unresolvable with an ion trap and cannot be included in our analysis. In Fig. 3, the relative intensities of radical directed backbone fragments that appear only in CAD of KIX radical species (i.e., they are not present in CAD of the corresponding even electron cation), are plotted as a function of sequence from charge states +6 through +12 and +16. In +8 and higher charge states, RDD fragments are primarily localized by sequence in close proximity to Tyr50, Tyr68–69 and Tyr77, which all correspond to potential radical initiating residues. At even higher charge states, fragmentation around Tyr50 becomes dominant, in agreement with the previous MALDI-MS data that suggested Tyr50 is the primary iodination site. However, the gradual disappearance of some RDD peaks in higher charge states is due to several factors: (i) less favored through-space radical migration in more extended structure, (ii) decreased dissociation threshold for mobile proton initiated competitive fragmentation channels, (iii) limited resolution for high charge state fragment ions in the LTQ linear ion trap. In CAD of KIX +16 radical protein, only RDD fragments around Tyr50 have sufficient signal intensities and resolution to allow assignment of charge state. This data does not rule out the possibility of small amounts of iodination at Tyr68–69 and Tyr77. Therefore, analysis of the compact structures will need to consider all three potential radical initiation points.

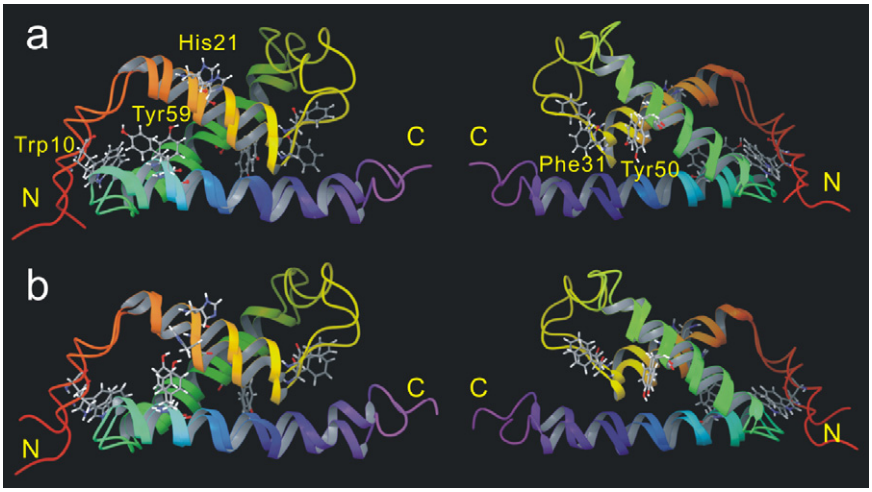

Fig. 4. Two local minima structures calculated by constraining and releasing distance pairs for +7 KIX in the gas phase overlapped with the native NMR structure. (a) Tyr59–Trp10 and Tyr50–Phe31 are proximate. RMSD is 3.4 Å. The picture on the right is the reverse viewpoint. (b) Tyr59–His21 and Tyr50–Phe31 are proximate. RMSD is 2.7 Å. N and C indicate the N- and C-termini, respectively.

Radical migration occurs only when kinetic and thermodynamic considerations are favorable. The kinetics are largely determined by structure, requiring that the radical donor has direct contact with the radical acceptor and that the relative orientation is favorable. The relevant C–H bond dissociation energies (BDEs) can generally be used to predict whether a reaction will be energetically favorable. The BDE of the C–H bond corresponding to the initial tyrosine radical generated by photodissociation is higher than most other non-aromatic hydrogens present in proteins, making hydrogen abstraction from most other residues exothermic. In other words, the initial tyrosine radical is highly reactive and will abstract hydrogen from most other C–H groups if the structure of the protein allows. Subsequent migrations are also possible, though less likely because the radical favors migration to more stable locations which become less abundant as the radical migrates downhill. The ultimate radical destination can be identified by assignment of the RDD fragments that are observed following activation of the protein radical, and connections with protein structure can be determined as explained previously [16].

RDD backbone fragments are typically initiated from a β-carbon radical in the side chain, which undergoes β-scission to cleave the adjacent C_α–C or N–C_α bond to generate a/x ions or c/z ions. Radical x ions will generally dissociate further into z or w ions.

3.3. Secondary structure

For the +8 through +11 charge states, one of the most abundant radical directed backbone cleavages is at residue Asn46 as shown in Fig. 3. Asn46 is four residues away from the primary initial radical site at Tyr50. Facile radical migration to an amino acid four residues away can be easily rationalized if the protein is α-helical in this region. The condensed phase structure reveals that Tyr50 and Asn46 are located in the α2 helix region. There are 3.6 residues per turn in an α helix, which places the side chain of Asn46 in close proximity to Tyr50 and allows abstraction of the β-hydrogen to proceed without distortion of the helical structure. This suggests that the secondary structure in this region is preserved when KIX is transferred from the solution phase to the gas phase in these charge states, as suggested previously [23]. In the +16 charge state, this fragmentation pathway is no longer favorable, indicating loss of α-helical structure in the higher charge states. The RDD results examining secondary structure are consistent with the data previously obtained for KIX by ECD [23].

3.4. Tertiary structure

As demonstrated previously, radical migration can also be used to examine protein tertiary structure [16]. Tertiary structural information is inferred from radical migrations which are distant in sequence from the initial residue where the radical is generated. These residues must be spatially proximate to the initial radical site in order for migration to occur, and therefore contain information about the three dimensional organization of the protein. These distance constraints can then be used to drive molecular dynamics simulations towards relevant conformational space and help evaluate potential structures. In the case of KIX, analysis of the RDD data is complicated slightly by the presence of multiple sites of iodination. In this situation, each dissociation endpoint must be considered in relation to several potential radical initiation sites. For evaluation of a known structure, agreement with the RDD data is determined by evaluating whether each radical endpoint is within proximity of any of the potential radical initiation points. Multiple radical initiation points will actually provide more diverse spatial proximity information which could in theory be better for probing a particular protein conformation. KIX has been reported previously to preserve the known solution structure in the gas phase for +7 and lower charge states [23]. Determining whether the RDD data is consistent with retention of the solution phase structure in the gas phase is therefore a fairly straightforward endeavor.

Backbone dissociation at favorable radical acceptor residues (i.e., Trp10, His21, and Phe31 which have side chains with low β C–H BDEs) which are sequence remote from tyrosine residues is most prevalent for the +6 charge state of KIX, as observed in Fig. 3. The RDD data for the +7 charge state appears to bridge the results for the +6 and +8 charge states, suggesting that a structural transition may take place at this charge state. Evaluation of the spatial proximity for the solution phase structure between iodinated tyrosine residues and sites of dissociation such as Trp10, His21, and Phe31 (8.2 Å, 7.6 Å, and 6.2 Å, respectively) are larger than would be expected for radical migration to be able to occur. However, local minima structures on the potential energy surface that are within 80 kJ/mol energy of the solution phase structure are easily obtained when these distances are reduced below 5 Å. The Trp10 and His21 sites represent different, mutually exclusive conformations where

Tyr69 can bind to one or the other, but not both simultaneously as can be seen in Fig. 4. The overall folds for both conformers are very similar to the solution phase structure with root mean square deviations (RMSD) of 3.4 Å and 2.7 Å for the structures in Fig. 4a and b, respectively. Based on the backbone atoms in α helical regions only, all structures are within an RMSD of 2.1 Å, suggesting that random coil regions are more flexible than α helices. Alternative folds were explored by constraining tyrosine residues to sites of dissociation in various combinations and subjecting these structures to simulated annealing from 2500 K to 50 K; however, no lower energy structures were obtained in this fashion. Furthermore, the solution phase three-helix bundle structure of KIX is stable when subjected to stochastic molecular dynamics simulations at 300 K for one nanosecond. Although this timescale may be too short to reflect potential structure changes that might eventually occur at longer timescales [28], the observed stability is in agreement with the RDD data acquired on the millisecond timescale. The influence of charge site selection was also investigated. The relative energies and conformations adopted by KIX are not extremely sensitive to choice of charge locations. This suggests that multiple protonation conformers may exist in reality, which may influence local structural preferences (e.g., binding of Tyr69 to Trp10 or His21).

Why is the gas phase structure of KIX similar to that found in solution? Favorable electrostatic contributions, including salt bridges, have been suggested previously and likely are important [23]. However, it is important to recognize that not all salt bridges present in solution can be retained in the gas phase. The body of work which has been done on the stabilization of charge separation in the gas phase (as is required for salt bridge formation) suggests that only arginine containing salt bridges will be stable in the gas phase [29–31]. The significantly reduced basicity of lysine in comparison makes salt bridge stabilization much more difficult to achieve. With that in mind, there are several salt bridges which should survive in the gas phase. In particular, the Arg19–Glu55 salt bridge is potentially important. This salt bridge is partially buried, suggesting structural importance in solution [32], and serves to anchor α1 to α2. In addition, the Arg42–Asp41 salt bridge may be important to stabilize α2. Alpha helices are known to be stable in the gas phase, particularly when a positive charge resides at the C-terminus [33]. The Arg42–Asp41 salt bridge is at the N-terminus of the α2 helix, and the salt bridge dipole is oriented to interact favorably with the macrodipole of the helix. Protonation of Arg42 in the absence of the salt bridge would destabilize the α2 helix. The C-terminus of α2 is stabilized with a proton by Lys8. In addition, a (net) protonated salt bridge may form between Arg90, the C-terminus, and Arg88. This salt bridge would anchor α3 by strongly connecting the terminal residues, and placing a positive charge in the proper location to interact with the helix macrodipole. This salt bridge may explain why α3 is the most stable helical region according to ECD [23]. Similarly, the lack of charge stabilization of the helix macrodipole may explain why α1 is the least stable helix. Charges which do not interact with the helices can be placed at several different locations due to the multiplicity of basic sites which are available in KIX. The large number of side chains with polar groups additionally helps to ensure that these charges can be solvated without significant rearrangement of the backbone.

4. Conclusions

Results obtained by radical directed dissociation are consistent with the KIX domain retaining a three-helix bundle structure in the gas phase which is very similar to the native structure determined by NMR in solution. The native structure is retained due to a combination of factors. KIX secondary structure is primarily alpha helical, a motif which has been demonstrated to be stable in the gas phase. The solvation of charge for the +6 and +7 charge states of KIX can be accommodated without significant structural rearrangement. Furthermore, there are numerous potential sites where the charges can be placed, increasing the likelihood that charges will be able to reside in locations that do not require structural rearrangement. There are also several key salt bridges and favorable ion-helix dipole interactions which likely help to hold the structure together in the gas phase once solvent has been removed.

Acknowledgments

The authors gratefully acknowledge funding from the National Science Foundation (CHE-074748). We also thank Kathrin Breuker and Martin Tollinger (University of Innsbruck) for kindly providing the KIX protein.

References

[1] C.-I. Brändén, J. Tooze, Introduction to Protein Structure, 2nd ed., Garland Pub., New York, NY, 2009.
[2] J.N. Sachs, D.M. Engelman, Introduction to the membrane protein reviews: the interplay of structure, dynamics, and environment in membrane protein function, Annu. Rev. Biochem. 75 (2006) 707–712.
[3] D.E. Clemmer, M.F. Jarrold, Ion mobility measurements and their applications to clusters and biomolecules, J. Mass Spectrom. 32 (1997) 577–592.
[4] J.R. Eyler, Infrared multiple photon dissociation spectroscopy of ions in penning traps, Mass Spectrom. Rev. 28 (2009) 448–467.
[5] M.E. Belov, M.V. Gorshkov, H.R. Udseth, G.A. Anderson, R.D. Smith, Zeptomole-sensitivity electrospray ionization-Fourier transform ion cyclotron resonance mass spectrometry of proteins, Anal. Chem. 72 (2000) 2271–2279.
[6] M. Han, M. Jin, K. Breuker, F.W. McLafferty, Extending top-down mass spectrometry to proteins with masses greater than 2*0*0 kilodaltons, Science 314 (2006) 109–112.
[7] K.J. Gillig, B. Ruotolo, E.G. Stone, D.H. Russell, K. Fuhrer, M. Gonin, A.J. Schultz, Coupling high-pressure MALDI with ion mobility/orthogonal time-of flight mass spectrometry, Anal. Chem. 72 (2000) 3965–3971.
[8] C. Uetrecht, I.M. Barbu, G.K. Shoemaker, E. van Duijn, A.J.R. Heck, Interrogating viral capsid assembly with ion mobility–mass spectrometry, Nature Chem. 3 (2011) 126–132.
[9] C. Bleiholder, N.F. Dupuis, T. Wyttenbach, M.T. Bowers, Ion mobility–mass spectrometry reveals a conformational conversion from random assembly to beta-sheet in amyloid fibril formation, Nature Chem. 3 (2011) 172–177.
[10] J.J. Thomas, B. Bothner, J. Traina, W.H. Benner, G. Siuzdak, Electrospray ion mobility spectrometry of intact viruses, Spectrosc. Int. J. 18 (2004) 31–36.
[11] D.E. Clemmer, R.R. Hudgins, M.F. Jarrold, Naked protein conformations—cytochrome-C in the gas-phase, J. Am. Chem. Soc. 117 (1995) 10141–10142.
[12] B.T. Ruotolo, K. Giles, I. Campuzano, A.M. Sandercock, R.H. Bateman, C.V. Robinson, Evidence for macromolecular protein rings in the absence of bulk water, Science 310 (2005) 1658–1661.
[13] D.M. Horn, K. Breuker, A.J. Frank, F.W. McLafferty, Kinetic intermediates in the folding of gaseous protein ions characterized by electron capture dissociation mass spectrometry, J. Am. Chem. Soc. 123 (2001) 9792–9799.
[14] R.B.J. Geels, S.M. van der Vies, A.J.R. Heck, R.M.A. Heeren, Electron capture dissociation as structural probe for noncovalent gas-phase protein assemblies, Anal. Chem. 78 (2006) 7191–7196.
[15] K. Breuker, H.B. Oh, D.M. Horn, B.A. Cerda, F.W. McLafferty, Detailed unfolding and folding of gaseous ubiquitin ions characterized by electron capture dissociation, J. Am. Chem. Soc. 124 (2002) 6407–6420.
[16] T. Ly, R.R. Julian, Elucidating the tertiary structure of protein ions in vacuo with site specific photoinitiated radical reactions, J. Am. Chem. Soc. 132 (2010) 8602–8609.
[17] T. Ly, R.R. Julian, Tracking radical migration in large hydrogen deficient peptides with covalent labels: facile movement does not equal indiscriminate fragmentation, J. Am. Soc. Mass. Spectrom. 20 (2009) 1148–1158.
[18] B.N. Moore, S.J. Blanksby, R.R. Julian, Ion-molecule reactions reveal facile radical migration in peptides, Chem. Commun. (2009) 5015–5017.
[19] Q.Y. Sun, S. Yin, J.A. Loo, R.R. Julian, Radical directed dissociation for facile identification of iodotyrosine residues using electrospray ionization mass spectrometry, Anal. Chem. 82 (2010) 3826–3833.
[20] P. Carter, Site-directed mutagenesis, Biochem. J. 237 (1986) 1–7.
[21] N. Vo, R.H. Goodman, CREB-binding protein and p300 in transcriptional regulation, J. Biol. Chem. 276 (2001) 13505–13508.
[22] R.N. De Guzman, N.K. Goto, H.J. Dyson, P.E. Wright, Structural basis for cooperative transcription factor binding to the CBP coactivator, J. Mol. Biol. 355 (2006) 1005–1013.
[23] K. Breuker, S. Bruschweiler, M. Tollinger, Electrostatic stabilization of a native protein structure in the gas phase, Angew. Chem. Int. Ed. 50 (2011) 873–877.
[24] W.L. Jorgensen, D.S. Maxwell, J. TiradoRives, Development and testing of the OPLS all-atom force field on conformational energetics and properties of organic liquids, J. Am. Chem. Soc. 118 (1996) 11225–11236.

[25] E. Polak, G. Ribiere. Note sur la Convergence de Méthodes de Directions Conjuguées. Revenue Francaise Informat. Recherche Operationelle, Serie Rouge, 1969, 16, 35.
[26] W. Yu, J.E. Vath, M.C. Huberty, S.A. Martin, Identification of the facile gas-phase cleavage of the Asp Pro and Asp Xxx peptide-bonds in matrix-assisted laser-desorption time-of-flight mass-spectrometry, Anal. Chem. 65 (1993) 3015–3023.
[27] B.L. Schwartz, M.M. Bursey, Some proline substituent effects in the tandem mass-spectrum of protonated pentaalanine, Biol. Mass Spectrom. 21 (1992) 92–96.
[28] M.Z. Steinberg, R. Elber, F.W. McLafferty, R.B. Gerber, K. Breuker, Early structural evolution of native cytochrome c after solvent removal, ChemBioChem 9 (2008) 2417–2423.
[29] R.R. Julian, R. Hodyss, J.L. Beauchamp, Salt bridge stabilization of charged zwitterionic arginine aggregates in the gas phase, J. Am. Chem. Soc. 123 (2001) 3577–3583.
[30] T. Wyttenbach, M. Witt, M.T. Bowers, On the question of salt bridges of cationized amino acids in the gas phase: glycine and arginine, Int. J. Mass Spectrom. 183 (1999) 243–252.
[31] J.S. Prell, J.T. O'Brien, J.D. Steill, J. Oomens, E.R. Williams, Structures of protonated dipeptides: the role of arginine in stabilizing salt bridges, J. Am. Chem. Soc. 131 (2009) 11442–11449.
[32] O. Schueler, H. Margalit, Conservation of salt bridges in protein families, J. Mol. Biol. 248 (1995) 125–135.
[33] R.R. Hudgins, M.A. Ratner, M.F. Jarrold, Design of helices that are stable in vacuo, J. Am. Chem. Soc. 120 (1998) 12974–12975.